Quantum-confined interband absorption in GaAs sawtooth-doping superlattices

E. F. Schubert, B. Ullrich,* T. D. Harris, and J. E. Cunningham†
AT&T Bell Laboratories, 600 Mountain Avenue, Murray Hill, New Jersey 07974-2070
(Received 10 June 1988)

Optical-interband-absorption experiments are performed on GaAs doping superlattices, which have sawtooth-shaped band-edge potentials. Absorption spectra reveal for the first time a clear signature of quantum-confined transitions and exhibit excitonic enhancement of the absorption. The maxima in the experimental absorption spectra are assigned to theoretical energies of quantum-confined transitions with very good agreement. The observation of quantum-confined transitions demonstrates the superiority of the new sawtooth structure over conventional doping superlattices.

Nineteen years ago, Esaki and Tsu[1] proposed to superimpose a periodic superlattice potential caused by alternating *n*-type and *p*-type dopants onto the crystal potential of an epitaxial semiconductor. This proposal initiated theoretical and experimental[2–7] work in the field of such doping superlattices. Extended and comprehensive reviews[3–5] have become available. Size quantization would be naively expected to occur in doping superlattices with sufficiently small periods. However, the high concentration of impurities in doping superlattices reduces the coherence length of carriers due to impurity scattering, possibly below the electron de Broglie wavelength. It is thus not clear if quantum-confined optical interband absorption can be observed at all in doping superlattices. To date, optical interband spectroscopy, has not revealed the quantum-confined nature of valence-subband to conduction-subband transitions.[3–5] In contrast to conventional doping superlattices, *compositional* superlattices [e.g., GaAs/(Al,Ga)As] allow unambiguous observation of quantum-confined interband transitions.[5,6]

In this paper we report on the first observation of quantum-confined, excitonic interband transitions in absorption measurements on GaAs sawtooth-doping superlattices. Although the sawtooth structure deviates from the originally proposed structure, this novel structure represents a significant improvement over conventional doping superlattices and thus allow us to observe excitonic quantum-confined transitions in doping superlattices. We will first describe the sawtooth structure[7] and calculate the subband structure employing the exact Airy-function solution. We will then present absorption spectra for temperatures 6–300 K and compare theoretical and experimental peak energies. Finally, we discuss the unique features of the absorption data, including excitonic enhancement of the absorption and the functional dependence of the absorption versus energy. We point out that the observation of quantum-confined excitonic transitions is of special importance, because it opens the area of quantum and excitonic effects to the field of doping superlattices.

It is desirable for doping superlattices to achieve a *large* periodic potential modulation on a *short* length scale. Which dopant distribution will result in the largest possible potential modulation at a *given period* z_p and a *given amount of dopants*? The answer to this question is illustrated in the doping profile shown in Fig. 1(a): The maximum potential modulation is obtained if the doping profile is a train of alternating Dirac delta functions separated by $z_p/2$.[7,8] The resulting conduction- and valence-band potential is sawtooth shaped, as shown in Fig. 1(b). This sawtooth structure allows us to obtain a potential modulation that is a factor of 2 larger than the potential modulation of conventional (*n-i-p-i*) doping superlattices. Diffusion of impurities in δ-doped GaAs is irrelevant, if the sample is grown under appropriate conditions.[9]

The exact calculation of eigenstate energies in a V-shaped potential well is obtained by transforming the

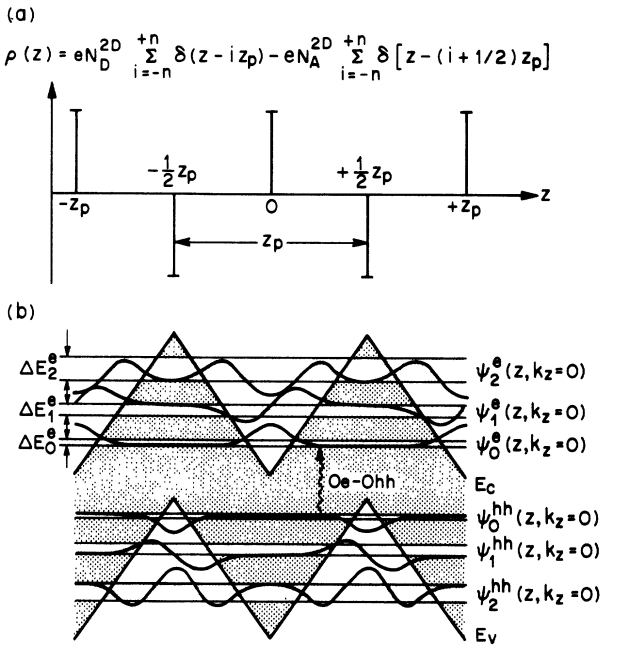

FIG. 1. (a) Charge distribution in a sawtooth superlattice with period z_p and doping concentration N_A^{2D} and N_D^{2D}. (b) Electronic band diagram of a sawtooth superlattice. The wave functions $\psi_n(z)$ are shown for $k_z=0$. Minibands have a width of ΔE_n.

Schrödinger equation into the Airy differential equation.[10–12] The V-shaped potential well is defined by $V(z)=Fz$ $(z>0)$ and $V(z)=-Fz$ $(z<0)$, where F is the electric field generated by the dopants and z is the spatial coordinate. We use the ansatz for even states,

$$\psi(z)=\begin{cases} c_1\mathrm{Ai}[\beta(z-\gamma)]+c_2\mathrm{Bi}[\beta(z-\gamma)] & (z>0) \quad (1a) \\ c_1\mathrm{Ai}[\beta(-z-\gamma)]+c_2\mathrm{Bi}[\beta(-z-\gamma)] & (z<0) \quad (1b) \end{cases}$$

and for odd states

$$\psi(z)=\begin{cases} c_1\mathrm{Ai}[\beta(z-\gamma)]+c_2\mathrm{Bi}[\beta(z-\gamma)] & (z>0) \quad (1c) \\ -c_1\mathrm{Ai}[\beta(-z-\gamma)]-c_2\mathrm{Bi}[\beta(-z-\gamma)] & (z<0) \quad (1d) \end{cases}$$

where c_i are constants, $\beta=(2m^*eF/\hbar^2)^{1/3}$, and $\gamma=E/(eF)$. Using appropriate boundary conditions yields $c_2=0$ and finally the subband energies. With an asymptotic expansion for the zeros of the Airy function and its derivative, one obtains

$$E_n=\left[\frac{3\pi}{4}(n+\tfrac{1}{2})\right]^{2/3}\left[\frac{\hbar^2e^2F^2}{2m^*}\right]^{1/3}, \quad n=0,1,2,\ldots . \quad (2)$$

To obtain the exact (nonasymptotic) subband energies the term $(n+\frac{1}{2})$ in Eq. (2) has to be replaced by 0.437,1.517,2.484,3.508 for $n=0,1,2,3$, respectively. It is worthwhile to point out that the first excited state $(n=1)$ of the V-shaped well coincides with the ground-state energy of the triangular well, which in turn is published in Ref. 13. We have also performed a variational calculation to determine the ground-state energy of the V-shaped potential well.[14] The extension of the solutions with Airy functions from a single V-shaped potential well to a sawtooth superlattice implies a splitting of individual subbands of energy E_n in minibands of width ΔE_n. However, the miniband width ΔE_0 is relatively small ($\Delta E_0<5$ meV) for the sample parameters used in this study. Thus, transition energies are obtained from Eq. (2) to a sufficient degree of accuracy.

Optical transitions in sawtooth superlattices are not governed by conventional selection rules, i.e., optical dipole matrix elements are finite and nonzero for all possible transitions. The matrix element involves an initial and final state which have an exponentially decaying part and a spatially oscillating part, as shown in Fig. 1, yielding a finite, nonzero transition probability for all transitions. This property of the sawtooth superlattice is in contrast to compositional superlattices where conventional selection rules do apply [e.g., $\Delta n=0$ for (Al,Ga)As/GaAs superlattices with no electric field present]. Optical transition energies are easily calculated using

$$E_{nm}=E_g^{\mathrm{GaAs}}-eV_z+E_n^e+E_m^{\mathrm{hh,lh}}, \quad (3)$$

where E_g^{GaAs} is the gap energy of the GaAs host lattice, eV_z is the modulation of the band edges $[eV_z=\frac{1}{2}Fz_p=\frac{1}{4}(e/\epsilon)N^{2\mathrm{D}}z_p]$ and E_n^e, e_m^{hh}, and E_m^{lh} are the subband energies of electrons, heavy holes, and light holes, respectively.

The GaAs epitaxial layers used for this study have been grown by gas-source molecular-beam epitaxy on undoped semi-insulating GaAs substrate. The growth temperature was kept below $T=550$ °C to avoid diffusion of n-type (Si) and p-type (Be) impurities.[8] Undoped GaAs samples have electron mobilities of 270 000 cm^2/V s at $T=40$ K. The design parameters of the superlattice include a period of $z_p=150$ Å and a two-dimensional doping concentration of $N_D^{2\mathrm{D}}=N_A^{2\mathrm{D}}=1.25\times10^{13}$ cm^{-2}. The samples have 10 periods of 20 dopant sheets separated by $\frac{1}{2}z_p=75$ Å. The samples have a closely balanced impurity concentration, i.e., $N_D^{2\mathrm{D}}\cong N_A^{2\mathrm{D}}$. Such a balance is essential, because its absence would blue shift the absorption edge according to the Burstein-Moss shift. Absorption measurements are performed on polished, 0.25-cm^2 samples. A dual-beam Perkin-Elmer Model 330 spectrophotometer and a variable-temperature cold-finger cryostat are used.

Results of absorption measurements on GaAs sawtooth superlattices measured at $T=6$ K are shown in Fig. 2. The gap energy of the undoped GaAs substrate corresponds to a wavelength of $\lambda=820$ nm and is shown by a double arrow. The substrate absorbs light at energies slightly below the fundamental gap; this absorption of bulk material is known as the Urbach tail.[15] We determined the corresponding Urbach-tail energy to be $E_U=6$ meV for our undoped GaAs samples. A typical absorption spectrum of a GaAs sample is shown as a dashed curve in Fig. 2.

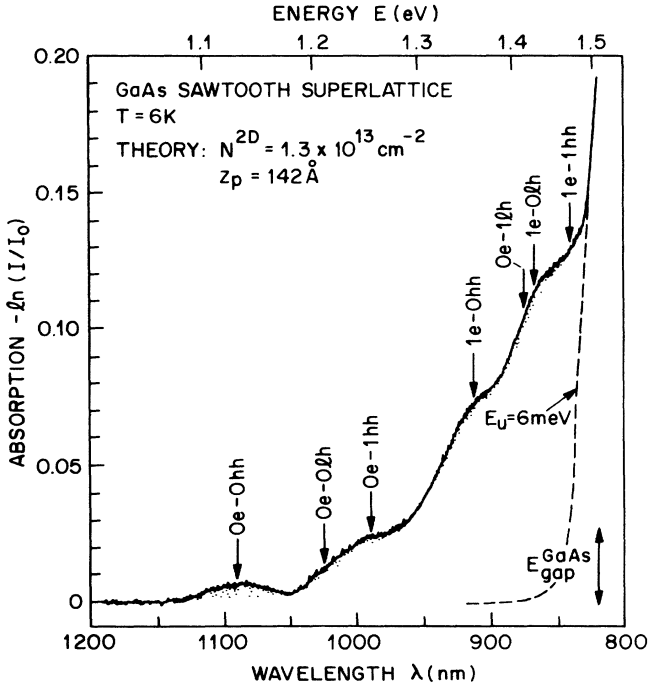

FIG. 2. Optical interband absorption spectrum of a GaAs sawtooth superlattice at $T=6$ K. Theoretical transition energies are indicated by arrows. The lowest electron to lowest heavy-hole transition is referred to as 0e-0hh. The parameters used for the calculation are a period of 142 Å and a dopant concentration of 1.3×10^{13} cm^{-2}. The energy gap of the substrate is marked by a double arrow. The absorption tail of the substrate is characterized by an Urbach-tail energy of $E_U=6$ meV.

The absorption spectrum shown in Fig. 2 shows strong absorption below the fundamental gap of GaAs in a range of 400 meV below the band gap of the GaAs host lattice. The most striking aspect of the absorption spectrum are four distinct features: an absorption maximum (peak) at $\lambda = 1090$ nm and three shoulders at wavelengths of $\lambda = 1000$, 920, and 865 nm. We attribute the structure to transitions between quantum-confined states in the valence and conduction band. Such quantum-confined interband transitions have not been observed since the invention of doping superlattices, 19 years ago. Furthermore, the absorption is not monotonically increasing with energy, but has a clear *peak* at $\lambda = 1090$ nm. Unlike the absorption spectrum shown in Fig. 2, the joint density of states is increasing *monotonically* with energy. The occurrence of such an absorption peak therefore shows the presence of excitonic or electron-hole correlation effects.

The formation of excitons necessitates a novel, extended understanding of physical properties of doping superlattices. According to previous beliefs, electron-hole separation[2-4] naturally objects to the formation of excitons. However, the result presented here elucidate exciton formation in sawtooth superlattices with appropriate design parameters. Furthermore, excitonic absorption increases the absorption coefficient by several orders of magnitude[16,17] over nonexcitonic absorption, which in turn has been observed in conventional doping superlattices.[1-5] Thus, the sawtooth superlattice provides unique physical properties not found in other structures or material systems.

The built-in electric field in the sawtooth superlattice is given by $F = eN^{2D}/2\epsilon$ which equals to $F \gtrsim 5 \times 10^5$ V/cm. At such high fields excitonic absorption is not observable in homogeneous semiconductors or square-shaped quantum wells[12] due to a field-induced ionization of excitons. In contrast to homogeneous semiconductors or square-shaped quantum wells, the sawtooth structure, even though an extremely high field is present, opposes a field-induced separation of carriers over more than half a superlattice period. Thus, electron-hole correlation effects are observed even at field strengths exceeding 10^5 V/cm. Excitonic enhancement of the absorption can, however, occur in doping superlattices, only if the spatial electron-hole separation [which is approximately $z_p/2$ for the $n=0$ states, see Fig. 1(b) for illustration] is smaller than the electron-hole interaction length (excitonic diameter). This condition is indeed satisfied for our samples with $z_p/2 = 75$ Å.

We now compare the experimental absorption data to theoretical transition energies inferred from Eqs. (2) and (3). The arrows shown in Fig. 2 are calculated energies of quantum-confined transitions. The lowest electron ($n=0$) to lowest heavy-hole ($n=0$) transition is referred to as 0*e*-0hh transition. Very good agreement between calculated quantum-confined transition energies and experimental ones is observed over a wide range of energies. For the calculation a period of $z_p = 142$ Å and a doping concentration of $N_D^{2D} = N_A^{2D} = 1.3 \times 10^{13}$ cm^{-2} has been used.

In Fig. 3 the absorption is plotted on a logarithmic scale versus energy. A linear relationship (straight line)

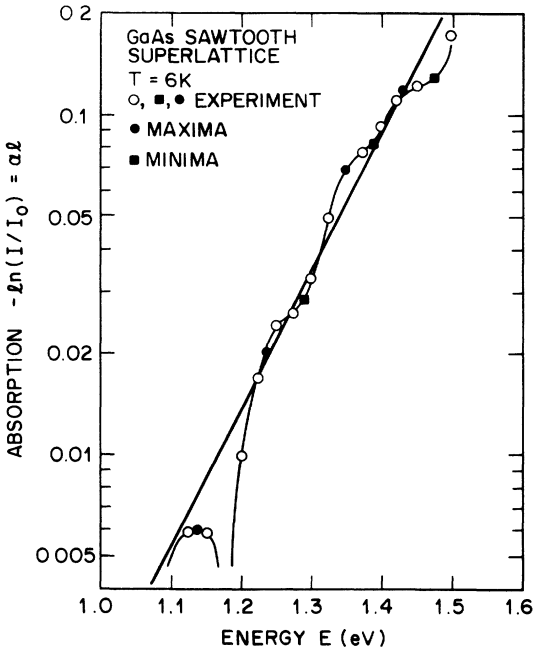

FIG. 3. Logarithmic absorption of a GaAs sawtooth superlattice at $T=6$ K vs photon energy. The quasilinear functional dependence (solid line) indicates a transition probability which increases exponentially with energy. Solid circles and solid squares represent maxima and minima of the absorption spectrum.

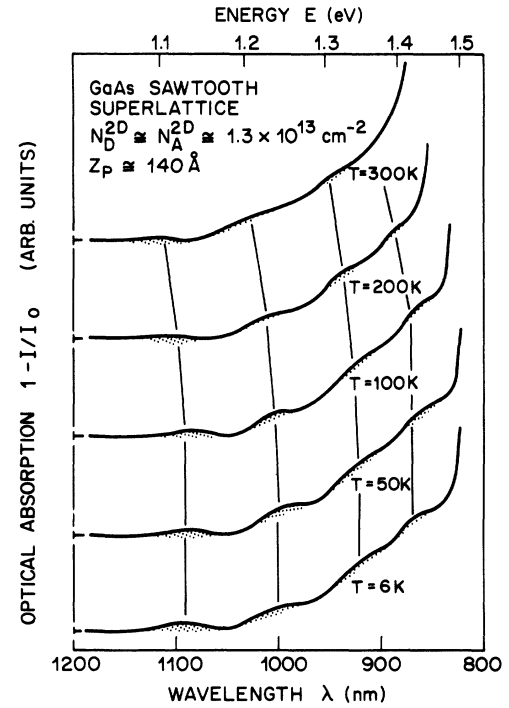

FIG. 4. Optical interband absorption of a GaAs sawtooth superlattice for sample temperatures $6 \leq T \leq 300$ K. A shift of the fundamental gap as well as the quantum-confined transitions is found with increasing temperature.

between the envelope of $\ln(\alpha l)$ and E is obtained.[17] Thus, an exponentially increasing transition probability with energy is inferred from Fig. 3. The envelope of the absorption is exponentially increasing due to an increasing overlap of wave functions and, accordingly, an exponentially increasing matrix element.

Additional absorption spectra for temperatures $6 \leq T \leq 300$ K are shown in Fig. 4. The absorption edge of the substrate shifts from 820 nm at $T=6$ K to 875 nm at $T=300$ K. The quantum-confined interband transitions of the sawtooth superlattice exhibit the identical qualitative shifts to longer wavelength as shown in Fig. 4. Such a shift of peak energies of the superlattice absorption is expected to track the shift of the band edge of the host material according to Eq. (5).

In conclusion, we have experimentally and theoretically studied optical interband absorption in a GaAs doping superlattice with a sawtooth-shaped conduction- and valence-band edges. Absorption measurements reveal for the first time quantum-confined interband transitions below the host-GaAs band-gap energy. The peak nature of the lowest transition ($n=0$) shows the presence of excitonic enhancement. The envelope of the absorption spectrum is an exponential function and reflects the increasing oscillator strength of the interband transition. Subband energies of a V-shaped potential well are calculated using Airy functions. Very good agreement is obtained between experimental absorption data and calculated subband energies. Quantum-confined transitions shift to lower energies at higher temperatures in agreement with the shift of the fundamental gap of the host GaAs semiconductor. The observation of quantum-confined transitions is made possible through the sawtooth structure which is superior to conventional doping superlattices. The measurement and the sawtooth structure reported here promise to be useful tools and of special importance in the area of superlattice research. The wide utilization and application of quantum effects as well as excitonic effects (which were and are so successful in compositional superlattices) can now be extended to the field of doping superlattice for research and technology.

The authors wish to thank L. C. Feldman, S. Schmitt-Rink, and H. L. Störmer for valuable discussions.

---

*Also at Max Planck Institut for Solid State Research, D-7000 Stuttgart 80, Federal Republic of Germany.
†AT&T Bell Laboratories, Holmdel, NJ 07733.

[1]L. Esaki and R. Tsu, IBM J. Res. Dev. **1**, 61 (1970).
[2]M. I. Ovsyannikov, Y. A. Romanov, V. N. Shabanov, and R. G. Loginova, Fiz. Tekh. Poluprovodn. **4**, 2225 (1970) [Sov. Phys.—Semicond. **4**, 1919 (1971)]; Y. A. Romanov, *ibid.* **5**, 1434 (1971) [*ibid.* **5**, 1256 (1972)].
[3]G. H. Döhler, H. Künzel, D. Olego, K. Ploog, P. Ruden, H. J. Stolz, and G. Abstreiter, Phys. Rev. Lett. **47**, 864 (1981); for a review, see G. H. Döhler, IEEE J. Quant. Electron. **QE-22**, 1682 (1986).
[4]K. Ploog and G. H. Döhler, Adv. Phys. **32**, 285 (1983).
[5]L. Esaki, IEEE J. Quant. Electron. **QE-22**, 1611 (1986).
[6]J. A. Brum, P. Voisin, and G. Bastard, Phys. Rev. B **33**, 1063 (1986).
[7]E. F. Schubert, Y. Horikoshi, and K. Ploog, Phys. Rev. B **32**, 1085 (1985).
[8]E. F. Schubert, J. E. Cunningham, and W. T. Tsang, Phys. Rev. B **36**, 1348 (1987).
[9]E. F. Schubert, J. B. Stark, U. Ullrich, and J. E. Cunningham, Appl. Phys. Lett. **52**, 1508 (1988).
[10]*Handbook of Mathematical Functions,* edited by M. Abramowitz and I. A. Stegun (National Bureau of Standards, Washington, D.C., 1964).
[11]E. J. Austin and M. Jaros, Phys. Rev. B **31**, 5569 (1985).
[12]H. X. Jiang and J. Y. Lin, J. Appl. Phys. **61**, 624 (1987).
[13]T. Ando, A. B. Fowler, and F. Stern, Rev. Mod. Phys. **54**, 437 (1982).
[14]A variational calculation with the trial functions $\psi_0(\pm z) = (2\alpha/5)^{1/2}(1\pm\alpha z)\exp(\mp\alpha z)$ for $(z \gtrless 0)$ yields a ground-state energy of $E_0 = \frac{3}{10}(9^2/2)^{1/3}[\hbar^2 e^2 F^2/(2m^*)]^{1/3}$. This energy is 1% higher than the energy of the Airy-function solution. [A variational calculation for a *triangular* well (not V shaped) has been performed by F. F. Fang and W. E. Howard, Phys. Rev. Lett. **16**, 797 (1966).]
[15]In 1953, Urbach established empirically the exponential dependence of the absorption coefficient of the photon energy near the long-wave fundamental absorption edge of alkali-halide crystals. This characteristic is not specific to alkali halides but is also found in other semiconductors. See F. Urbach, Phys. Rev. **92**, 1324 (1953).
[16]D. A. B. Miller, D. S. Chemla, and S. Schmitt-Rink, Phys. Rev. B **33**, 6976 (1986).
[17]A linear $\ln(\alpha l)$ versus E and $\ln(\alpha l)$ versus $E^{3/2}$ relationship is found in homogeneous GaAs subject to an electric field for excitonic and nonexcitonic absorption, respectively. See J. D. Dow and D. Redfield, Phys. Rev. B **1**, 3358 (1970).

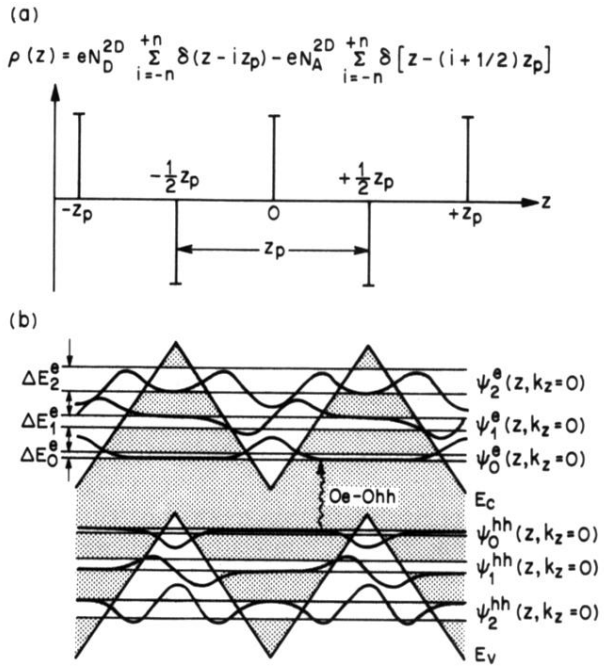

FIG. 1. (a) Charge distribution in a sawtooth superlattice with period z_p and doping concentration N_A^{2D} and N_D^{2D}. (b) Electronic band diagram of a sawtooth superlattice. The wave functions $\psi_n(z)$ are shown for $k_z=0$. Minibands have a width of ΔE_n.

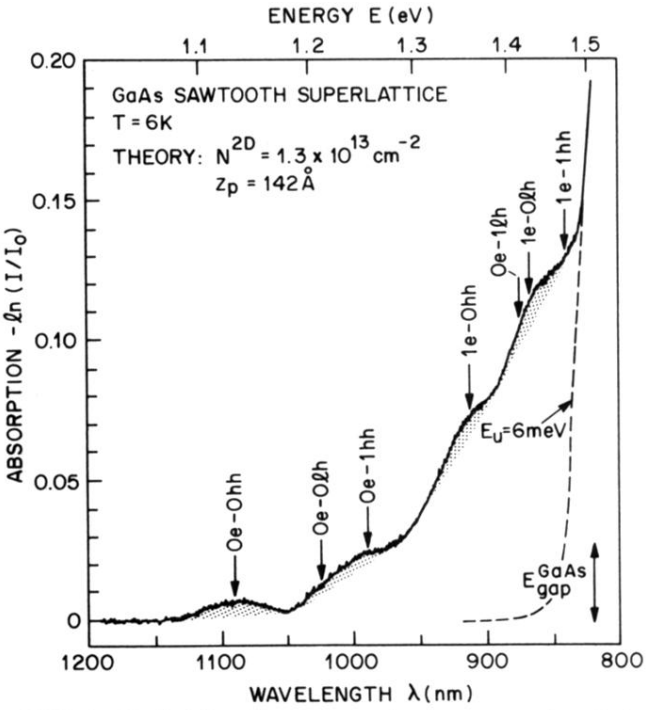

FIG. 2. Optical interband absorption spectrum of a GaAs sawtooth superlattice at $T=6$ K. Theoretical transition energies are indicated by arrows. The lowest electron to lowest heavy-hole transition is referred to as 0*e*-0hh. The parameters used for the calculation are a period of 142 Å and a dopant concentration of 1.3×10^{13} cm^{-2}. The energy gap of the substrate is marked by a double arrow. The absorption tail of the substrate is characterized by an Urbach-tail energy of $E_U=6$ meV.